

Available online at www.sciencedirect.com

ScienceDirect

journal homepage: www.elsevier.com/locate/he

Investigation on favourable ionic conduction based on CMC-K carrageenan proton conducting hybrid solid bio-polymer electrolytes for applications in EDLC

N.K. Zainuddin^a, N.M.J. Rasali^a, N.F. Mazuki^a, M.A. Saadiah^{a,b},
A.S. Samsudin^{a,*}

^a Ionic Materials Team, Faculty of Industrial Sciences and Technology, Universiti Malaysia Pahang, 26300 Pahang, Malaysia

^b Department of Chemistry, Centre for Foundation Studies, International Islamic University Malaysia, 26300 Gambang, Pahang, Malaysia

HIGHLIGHTS

- Proton conducting biopolymer electrolytes was prepared based CMC-KC doped NH_4NO_3 .
- H^+ which originate from H^+-NH_3 group of NH_4NO_3 act as carriers for conducting ions.
- The room temperature ionic conductivity achieved the maximum value at $\sim 10^{-4}$ S/cm.
- The H^+ ions contributes toward the enhancement of amorphous phase.
- The EDLC fabricated exhibited favourable electrochemical characteristics.

ARTICLE INFO

Article history:

Received 4 September 2019

Received in revised form

2 January 2020

Accepted 6 January 2020

Available online xxx

Keywords:

Hybrid polymer

H^+ carrier

Ionic conductivity

Electrochemical properties

ABSTRACT

In the present work, a proton-conducting hybrid solid biopolymer electrolytes (HSBEs) system was successfully prepared via the solution casting approached. The HSBEs comprised of CMC blended with kappa carrageenan and doped with NH_4NO_3 . The HSBEs system was characterized to evaluate the structural and the proton conduction properties using FTIR, XRD and EIS techniques. The FTIR analysis showed that a complexation occurred between the CMC-KC and H^+ moiety of the NH_4NO_3 via the $-\text{OH}$, $\text{C}-\text{O}-\text{C}$ as well as $-\text{COO}^-$ groups with associated changes observed to their wavenumbers and peak intensities. At the 80:20 ratio of the CMC:KC hybrid system, the optimum value of the ionic conductivity was found to be $\sim 10^{-7}$ S/cm. However, the addition of 30 wt % of NH_4NO_3 to the system markedly increased the ionic conductivity to $\sim 10^{-4}$ S/cm due to the increase in the amorphous phase in the HSBEs system as revealed by the XRD analysis. Meanwhile, the IR-deconvolution approach revealed an increase of the protonation (H^+) from NH_4NO_3 towards the co-ordinating site on the hybrid CMC-KC system and this in turn, led to the increment in the ionic mobility and diffusion of ions for transportation. An EDLC was fabricated using the highest conducting HSBEs sample developed in the present study and it exhibited favourable characteristics as a capacitor with a reasonably good stability with regards to its electrochemical properties.

© 2020 Hydrogen Energy Publications LLC. Published by Elsevier Ltd. All rights reserved.

* Corresponding author.

E-mail address: ahmadsalihin@ump.edu.my (A.S. Samsudin).

<https://doi.org/10.1016/j.ijhydene.2020.01.038>

0360-3199/© 2020 Hydrogen Energy Publications LLC. Published by Elsevier Ltd. All rights reserved.

Introduction

Research on energy devices based on safe materials has gained due attention, primarily owing to the concerns related to global warming and the energy crisis. In 1989, the first electrical double layer capacitor (EDLC), also known as the supercapacitor was developed [1–5]. The EDLC can be used in numerous applications such as in electric or hybrid vehicles as the energy device. The development of energy devices has shifted to liquid-based electrolytes, as it could deliver high conductivity and demonstrates excellent electrochemical properties. Nonetheless, the use of liquid-based electrolytes has its disadvantages. Corrosion of the electrodes from the reaction process and leakages that are harmful to humans as well as the environment are some of the disadvantages that underline their inappropriateness for electrochemical device applications [6,7]. Based on this viewpoint, many researchers are developing new and safer materials by exploring the potential use of polymers as polymer electrolytes (PEs) to replace the conventional liquid-based electrolytes. Much of the current literature on PEs pay particular attraction to the petrochemical-based polymers and some of the well-known are synthetic polymer materials which has been used during the preparation. However, some of the synthetic polymer are hazardous, non-biodegradable as well as high cost and harmful to environment and humankind. For these reason, countless determinations have been developed including the usage of natural and biodegradable resources. This is one of the effort and could be an alternate to replace the synthetic polymer due to its abundancy, non-hazardous properties and good biocompatibility [8].

To date, a considerable amount of effort has been carried out to enhance the properties of PEs such as by using mixed dopants and the addition of fillers. Nonetheless, low ionic conductivity that leads to unstable electrochemical properties when applied to energy storage was often reported. However, enhancement of the electrochemical properties in the PEs system by using the polymer blend technique has been established to produce better performance in comparison to the single type polymers. Through the implementation of the polymer blend method, no phase separation is exhibited with regards to their miscibility, which consequently increases the performance of such PEs [9–11]. Polymer hybrids or blends such as starch-chitosan [9]; poly (vinyl chloride) (PVC)-poly (ethyl methacrylate) (PEMA) [12] and polyvinyl alcohol (PVA)-polyethylene oxide [13] are some of the polymer hybrids that have been explored for PEs in the literature. Development of this blended polymer is very promising and regarded as evolutionary research due to the blend's versatility of being able to offer more coordinating spots, which expand the flexibility chain and their mobility, thus, leading to an increment of the conduction properties.

Since the 1980's, proton-conducting polymer electrolytes has been explored and investigated for use in electrochemical devices [14,15]. It should be noted here that the charge carriers are H^+ ions that originate from inorganic acids or ammonium ions whilst the passage of the H^+ ions occurs over the

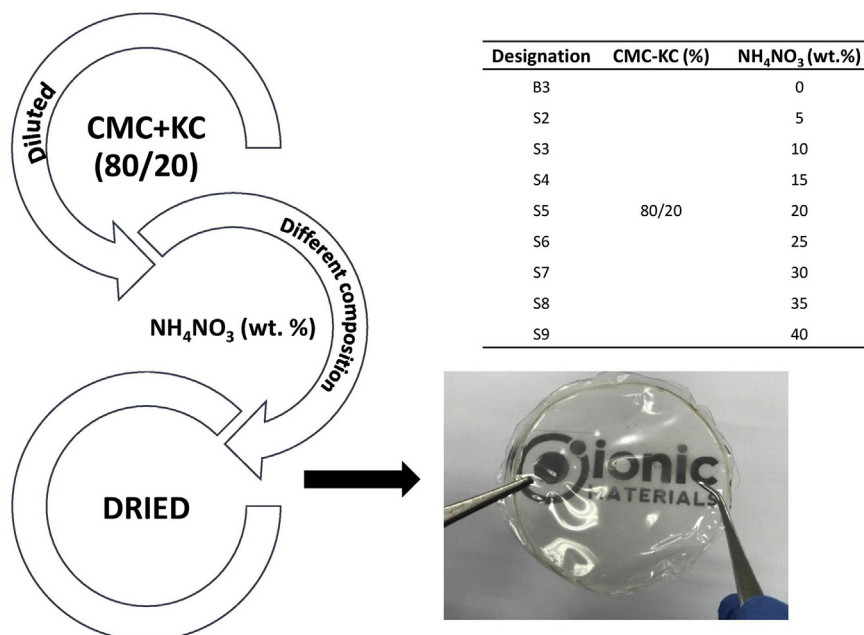
interchange of H^+ between co-ordinating sites in the polymer host [16,17]. It has been established from the literature that ammonium salts are promising candidates to act as an ionic dopants in PEs for energy device applications due to their low cost, compatibility to accommodate with polymers, favourable conductivity and thermal stability [18]. This is due to the ability of the NH_4^+ cations to be dominant charge carriers that enhances their electrochemical properties [19,20].

Hence, this work investigated the potential of carboxymethyl cellulose (CMC)-kappa carrageenan (KC) as a polymer host and NH_4NO_3 as an ionic dopant in a new family of hybrid solid biopolymer electrolytes (HSBEs) based on natural polymers. CMC and KC are categorized as anionic polysaccharide hydrophilic polymers and were chosen as the main elements for hybridization due to their outstanding characteristics, including being non-toxic materials, biodegradable, the most abundant organic substance on Earth, inexpensive and possess good film-forming characteristics [21]. In addition, we have already reported an optimum conductivity of $\sim 10^{-7}$ S/cm for a blended polymer CMC-KC based PEs system in a previous study [22]. As a continuation of our previous work, we now report the effects of adding NH_4NO_3 into the CMC-KC HSBEs system with an aim to explore the performance of the resultant potential of CMC-KC for fabrication as an EDLC device. The influence of H^+ carrier from the dopant system in HSBEs were characterized with regards to its structural and ionic conduction properties by using X-ray diffraction (XRD), Fourier Transform Infrared (FTIR) spectroscopy and electrical impedance spectroscopy (EIS). In addition, the deconvolution approach is applicable to both Arrhenius and non-Arrhenius behaviour in PEs was employed to examine the outcome of polymer blend-dopant material composition. The investigation was focusing on the variation of transport parameters in order to reveal favourable ionic mobility. The highest conducting sample was then fabricated into an EDLC device and tested with cyclic voltammetry and charge-discharge for evaluating their electrochemical properties. Findings from this work will act as baseline studies for further research which bring to the new perspective in proton conducting polymer electrolytes application towards green energy system.

Material and methods

Sample preparation of HSBEs film

In the present system, HSBEs film was prepared by using the solution casting technique. Based on our previous work [22], a 80:20 ratio of CMC: KC (Acros Organics Co and Shanxi Orient Co., respectively) was found to be the most favourable ratio for hybrid polymer electrolytes and this mixture was first dissolved in distilled water. Then, various amounts (5–40 wt %) of NH_4NO_3 (Merck Co.) were added into the CMC-KC solution and stirred until it became homogeneous. The homogenous solutions of CMC-KC- NH_4NO_3 were then casted into Petri dishes and left to dry at room temperature for a month to



Scheme 1 – Summary of sample preparation and their designation.

obtain the desired films. The prepared samples were kept in a desiccator filled with silica gels for further drying. Scheme 1 shows the preparation diagram and sample designations of HSBEs.

Characterization of HSBEs

Fourier transforms infrared spectroscopy (FTIR)

To identify the effect of NH₄NO₃ in the CMC-KC hybrid polymer, a Perkin Elmer 100 Fourier Transform Infrared (FTIR) spectroscope with an attenuated total reflection (ATR) accessory equipped with germanium crystal was used. The sample was tested within the frequency range of 4000 to 700 cm⁻¹ with a resolution of 2 cm⁻¹.

X-ray diffraction (XRD)

The XRD pattern of the CMC/KC-NH₄NO₃ HSBEs system was generated using a Rigaku MiniFlex II Diffractometer. The samples were first cut into 4 cm² sized portions and then pasted onto a sample slide. The prepared samples were then scanned using CuK_α as the radiation source at 2θ between 5° and 80°.

Electrical impedance spectroscopy (EIS)

The ionic conductivities of the prepared samples were tested by using a HIOKI 3532-50 LCR Hi-Tester with a frequency and temperature range of 50 Hz to 1 MHz and 303 K–343 K, respectively. The ionic conductivity, σ of the HSBEs samples were calculated based on the following equation:

$$\sigma = \frac{b}{R_b a} \quad (1)$$

where R_b is bulk resistance which was obtained from the Nyquist plot of imaginary impedance (Z_i) versus real impedance part (Z_r), b is the thickness of the electrolyte, and a is the contact area (cm²).

Voltammetry measurement

Linear sweep voltammetry (LSV) characteristics were measured using a C–H instrument potentiostat to study the potential windows of the HSBEs samples. Electrodes based on stainless steel were used as counter, working and reference electrodes and the samples were tested at a scan rate of 2 mV/s at room temperature with a voltage range of 0–3 V.

EDLC fabrication and characterization

In the construction of an electrical double-layer capacitor (EDLC) for applications in electrochemical devices, activated carbon, BP20, conducting carbon, super P and PVDF in the ratio of 80:15:5 were used as the primary materials for electrode preparation and were thoroughly mixed. The mixture was stirred by adding 4 mL of NMP in order to obtain a slurry. The slurry was then spread onto the current collector (aluminium sheet). The electrode was then heated at 100 °C in a vacuum oven for 24 h before being used. The HSBEs with the highest ionic conductivity was chosen as the electrolyte system for the EDLC device and was sandwiched between the two electrodes and then placed inside the coin cell. The fabricated EDLC was then tested for cyclic voltammetry (CV) using an Autolab PGSTAT M101. The CV analysis was measured at different scan rates with applied electrical potential of 0–1 V. The specific capacitance, C_s of the EDLC from CV plot was calculated using the following equation:

$$C_s = \int_{V_1}^{V_2} \frac{I(V)dV}{2(V_2 - V_1)m} \quad (2)$$

where $I(V)$ is the area under the graph, m is the mass of active material, $(V_2 - V_1)$ is the working potential voltage. The galvanostatic charge-discharge (GCD) was used to evaluate the electrochemical performance of the prepared EDLC cell. Charge – discharge measurement was done using a NEWARE

BTS battery cycler with a voltage from 0 to 1 V at different applied current density. The electrochemical properties of the EDLC based on the charge-discharge profile, namely C_s of specific capacitance, equivalent series resistance (ESR) and the Coulombic efficiency were calculated using equations found in the literature [23,24].

Results and discussion

FTIR analysis

FTIR is a powerful tool to analyze the complexation between the host polymer and salt, as well as to further understand the conduction mechanism of the developed HSBs. Fig. 1 shows the spectra of the CMC-KC HSBs system that was doped with different compositions of NH_4NO_3 in the 800–4000 cm^{-1} region. In this present research, the highlighted ATR-IR spectra of the complexation or interaction are discussed in Fig. 2. Based on the figure, the spectra for $-\text{O}-\text{SO}_3$ stretching, $\text{C}-\text{O}-\text{C}$ bending, $\text{O}=\text{S}=\text{O}$ symmetric, $\text{O}-\text{H}$ bending and COO^- asymmetrical spectra corresponded to the following bands: 846 cm^{-1} ; 928 cm^{-1} and 1024 cm^{-1} ; 1258 cm^{-1} ; 1322 cm^{-1} and 1582 cm^{-1} respectively.

Based on Fig. 2 (a), the interaction between the $-\text{O}-\text{SO}_3$ stretching vibration and symmetric bending (NH_4^+) could be observed at the 846 cm^{-1} wavenumber. The intensity of this peak shifted to lower wavenumbers and eventually disappeared as more NH_4NO_3 was incorporated into the system, while the band peak at 828 cm^{-1} (S9) began to appear. The intensities of the peaks were observed to decrease as the salt compositions increased, implying that there transpired interactions of both anions and cations of the CMC-KC- NH_4NO_3 complexes with polar groups. The interaction caused a charge inequality in the complexes and thus limited the bond

vibrations of the polar groups. The quaternary ammonium salt is regarded as a good source of protons since one of the H attaches to the NH_4^+ through a coordinate covalent bond which is weaker than ordinary covalent bonds and causes easier deprotonation. Moreover, the shifted wavenumber indicated that an interaction between the CMC-KC and NH_4NO_3 had occurred due to the migration (protonation) of H^+ from NH_4^+ towards the $\text{O}-\text{S}-\text{O}_3$ moiety in CMC-KC. This was due to the favourable hydrogen bonding interaction formed with the oxygen that carries available lone pairs of electrons in the group [25]. This also might be due to the increasing occurrence of hydrogen bonding between the sulphate group ($\text{O}-\text{S}-\text{O}_3$) of KC and the free proton of the dissociated NH_4NO_3 . The dissolution of the NH_4NO_3 in a hybrid polymer matrix provides ions which serve as charge carriers that contribute to the ionic conductivity under the influence of an electric field [26].

Fig. 2 (b) shows the ATR-IR mode at 928 cm^{-1} (B3) and 1024 cm^{-1} (B3) which were ascribed to the $\text{C}-\text{O}-\text{C}$ bending of the CMC-KC of the hybrid polymer. These two band peaks downshifted to lower wavenumbers of 925 cm^{-1} (S9), and 1043 cm^{-1} (S9). Meanwhile, the $\text{C}-\text{O}-\text{C}$ bending became more apparent and began to disappear due to the increase of NH_4NO_3 composition. This observation could be due to the presence of oxygen as the anionic polysaccharide in the CMC-KC hybrid polymer has a high affinity towards proton ions. It is believed that the H^+ ions from NH_4^+ have a tendency to interact with electron co-ordinating groups (O^-) in the hybrid biopolymer chains. These cross-linkage bonds impede the rotation of polymer segments, leading to the thickening of the biopolymer hybrid chains and in turn, lowering the energy barrier to the segmental movement which is reflected by the increment in number free ions [27]. Furthermore, the changes of intensity at the $\text{C}-\text{O}-\text{C}$ group could also be attributed to either occurrence or non-occurrence of H^+ protonation, which in turn is expected to affect the ionic conductivity values and the crystallinity of HSBs.

Fig. 2(c) shows the presence of bands at 1258 cm^{-1} and 1322 cm^{-1} that corresponded to the symmetric vibration $\text{O}=\text{S}=\text{O}$, and bending $\text{O}-\text{H}$ respectively. It was observed that the $\text{O}=\text{S}=\text{O}$ band of KC disappeared after the addition of 30 wt % of NH_4NO_3 , which implied the possible interaction between H^+ ions and oxygen atoms of the CMC-KC polymer chain complexes [28]. The disappearance of the co-ordinating site ($\text{O}=\text{S}=\text{O}$) with the introduction of the dopant might be due to the interactions that occurred in the HSBs with the inclusion of NH_4NO_3 . It can be seen that the peak at 1322 cm^{-1} of the undoped CMC-KC hybrid biopolymer blend sample (B3) assigned to the hydroxyl group ($-\text{OH}$) had shifted to the higher value of 1328 cm^{-1} with the inclusion of NH_4NO_3 . The peak changes at this value could be due to the interaction that occurred between the hydroxyl group ($-\text{OH}$) in CMC-KC and the amine group ($-\text{NH}_2$) band of the NH_4NO_3 when the ionic dopant was introduced. As reported by Kamarudin et al. [29], the $\text{O}-\text{H}$ band of CMC, which was found at $\sim 1320 \text{ cm}^{-1}$ shifted to higher wavenumbers as the dopant composition increased. According to them, this is evidence of the interaction between H^+ and the hydroxyl group. Complexation occurred due to lone proton migration, or protons carried the migration mechanisms between the oxygen of the hydroxyl group ($-\text{OH}$) in CMC-KC and H^+ ion of the ionic dopant NH_4NO_3 .

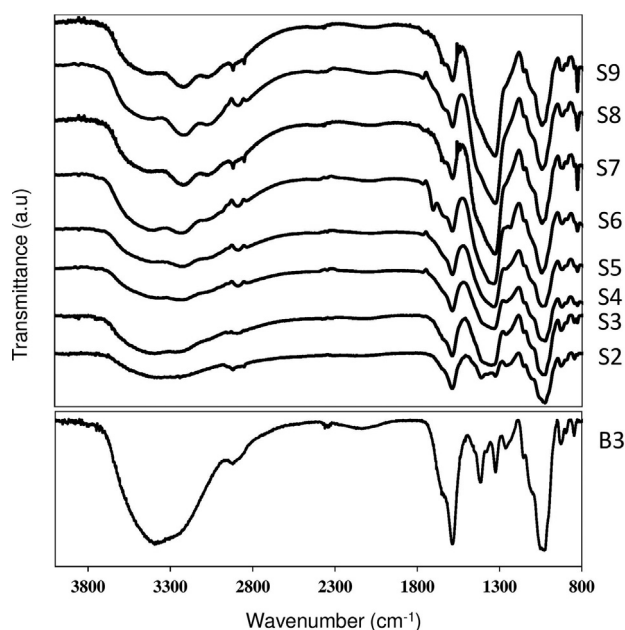


Fig. 1 – ATR-IR spectra of the CMC-KC doped with NH_4NO_3 at the 800–4000 cm^{-1} region.

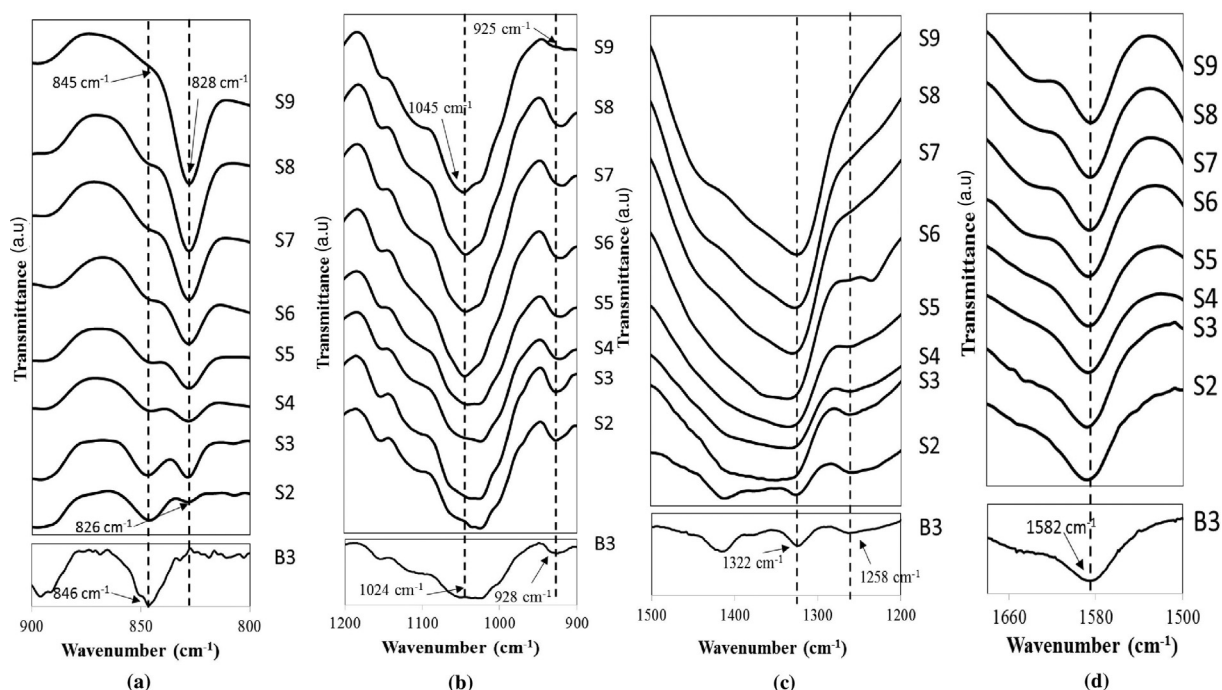


Fig. 2 – Highlighted ATR-IR spectra of the CMC-KC doped with NH_4NO_3 .

Fig. 2(d) depicts the characteristic band at 1582 cm^{-1} , which was attributed to the asymmetrical COO^- of the carboxylate anion group in the CMC-KC HSBs. It was apparent that the peak at 1582 cm^{-1} of sample B3 shifted to a higher wavenumber at 1585 cm^{-1} after the inclusion of 5 wt% of NH_4NO_3 , and the wavenumber increased to 1590 cm^{-1} when added with 30 wt% NH_4NO_3 . Then, the peak re-shifted to a lower wavenumber at 1582 cm^{-1} with 40 wt% of NH_4NO_3 . This observation is somewhat anticipated from the previous analysis. The functional group of C=O from CMC-KC would have significant complexation where this band had a strong bond with any cation introduced in the CMC-KC hybrid system. The complexation between the cations of H^+ dissociated from NH_4NO_3 in the co-ordinating site (C=O) from the CMC-KC hybrid polymer caused the peaks to shift to a higher wavenumber [30].

The peak shifts to higher wavenumbers were due to the stretching vibration of C=O as the electrons being reclusive from the C=O moiety to form strong hydrogen bonding in the CMC-KC hybrid polymer complexes. As the NH_4NO_3 increased, more NH_4NO_3 were dissolved, and more H^+ were dissociated. Since the flexibility of CMC-KC hybrid backbone had increased, the H^+ would easily interact with the C=O group. It can be noted here that H^+ ions were weakly coordinated to the carboxyl group, the cations were more mobile and thus, could be transported easily from one coordinating site to another [2]. The vibrational mode of pure NH_4NO_3 (~ 1500) can be assigned for vibrational band (NH_4^+) ion [31,32]. The interaction of H^+ from the NH_4NO_3 could be attributed to the coordination of the NH_4^+ ion when one of these H^+ ions jumped to the nitrogen atom that easily dissociated under the impact of an electric field. The protonated H^+ ions obeyed the Grotthuss mechanism where the ions migrated through a leap to the adjacent empty site, hence assisting the

conduction operation [33]. Apparently, the H^+ provided by NH_4NO_3 has greater tendency to be complexed with the CMC-KC as the latter could provide more complexation sites including the C-O-C , O=S=O and -COO^- groups which were susceptible for the proton conduction mechanism. According to Hema et al. [34] the strength of one H attaches to nitrogen (N) is weakly bonded compared to the other three bonds. This will drive N-H dissociation under the application of DC electric field and produce H^+ making it to be reliable resources. Previous work done by other researchers also support this finding where NH_4^+ is a good proton provider to the polymer electrolytes [35,36].

XRD analysis

The XRD patterns of CMC-KC hybrid solid biopolymer electrolytes (HSBEs) system with different compositions of NH_4NO_3 are shown in Fig. 3. In the present system, the incorporation of NH_4NO_3 assisted the biopolymer hybrid to be more amorphous. From Fig. 3, the semi-crystalline hump could be observed at $\sim 22.02^\circ$ (sample B3), and it was apparent that as the composition of NH_4NO_3 increased, the peak became more widened, demonstrating that the interaction had occurred between CMC-KC and NH_4NO_3 . This observation revealed the increment of the amorphous phase in the CMC-KC upon introduction of NH_4NO_3 , suggesting the increment of protonation of (H^+) in CMC-KC hybrid polymer due to the amorphous phase and thus resulting in the enhancement of ionic conductivity of the present system.

It can be seen that the amorphousness of the HSBs system began to decrease with the addition of more than 30 wt % of NH_4NO_3 . The presence of peaks at $2\theta = \sim 22.32^\circ$, $\sim 22.72^\circ$ and 27.1° , as shown in Fig. 3 for sample S8 and S9 implied that the hybrid polymer could no longer solvate the NH_4NO_3 . This may

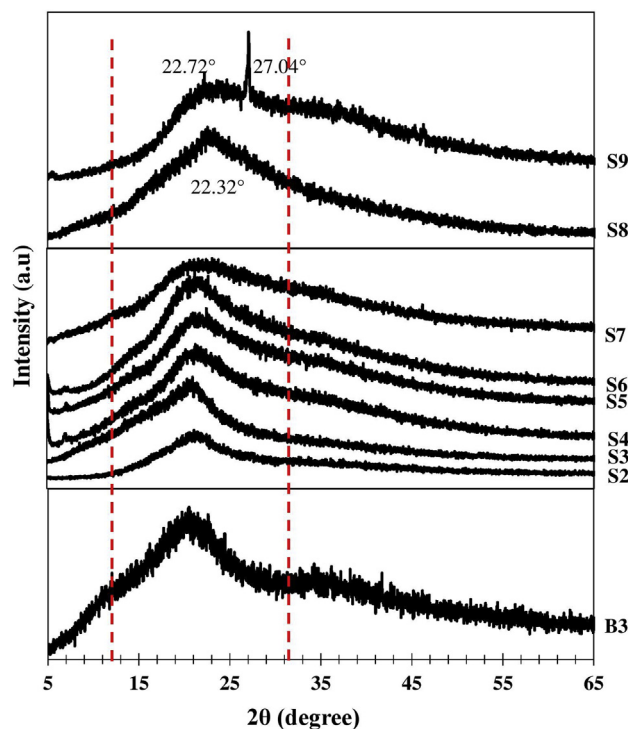


Fig. 3 – XRD spectra of the CMC-KC HSBES system that was doped with NH_4NO_3 .

be due to the occurrence of deprotonation where the excess NH_4NO_3 was not entrapped in the biopolymer blend. This would lead to its deposition on the surface of the film. The inability of the biopolymer host to accommodate the NH_4NO_3 resulted in the recombination of the ions and recrystallization of the dopant out of the film surface and contributed to the loss of a significant amount of mobile ions that affects the transport properties and conductivity [37].

Ionic conductivity analysis

The ionic conductivities of the CMC-KC- NH_4NO_3 HSBES system at ambient temperature are presented in Fig. 4. Based on our previous report [22], the value of conductivity for undoped CMC-KC (sample B3) HSBES system was 3.19×10^{-7} S/cm which was attributed to the enhancement of flexibility of polymer blend chain. In addition, CMC-KC blended polymer possesses conjugated double bonds at the CMC and KC backbone which can induced the electrical conductivity. Similar observation was obtained by previous research who disclosed the conductivity of biopolymer due to the conjugation phenomenon which provide charges through the electronic delocalization of the polymer backbone [38,39]. On top of that, the occurrence of conductivity value could be due to the segmental motion and polymer chain flexibility which contributed to the increased ionic mobility and this present work is similar as reported by other research work [5,7]. The ionic conductivity began to increase towards a higher value through doping with NH_4NO_3 . The dependence of ionic conductivity on the NH_4NO_3 composition provided information on specific complexation between the NH_4NO_3 and the CMC-KC biopolymer hybrid matrix as revealed by the FTIR and

XRD analysis. The increase of ionic conductivity in the CMC-KC- NH_4NO_3 HSBES system may be attributed to the ion dissociation of H^+ from $\text{NH}_4^+ - \text{NO}_3^-$ which interacted with the CMC-KC backbone and the increase in its transport properties [19,40]. In the CMC-KC- NH_4NO_3 HSBES system, there were more sites on the CMC-KC hybrid backbone where ion hopping from H^+ and exchange can take place, leading to higher ionic conductivity. Moreover, the XRD spectra also showed that the increment of the amorphous phase in the HSBES system led to the improvement in the ionic conductivity.

It is evident from Fig. 4 that the ionic conductivity achieved the maximum value of 2.00×10^{-4} S/cm for sample containing 30 wt% of NH_4NO_3 . This ionic conductivity value (10^{-4} S/cm) is adequate for use in electrochemical devices [41,42]. This observation proved that the blending method has a good potential in electrochemical device applications. However, above 30 wt % of NH_4NO_3 , the ionic conductivity of the HSBES system started to decrease. The decreasing value of ionic conductivity could be ascribed to the re-association of the H^+ carrier that turned into neutral ion cluster aggregates [43,44]. In addition, this observation could also be due to the recrystallization of the CMC-KC HSBES as revealed by the XRD analysis, which leads to an increase in the energy barrier for the segmental motion, thus decreasing the ionic conductivity.

Fig. 5 shows the plot of log conductivity, σ , versus $1000/T$ for the HSBES samples. It was noticeable that the ionic conductivity did not show any drastic leap with temperature, suggesting that there was no phase transition in the HSBES structures in the particular temperature range. As can be seen in Fig. 5, ionic conductivity increased with temperature including in the un-doped sample, which is associated with the increase in chain flexibility and revealed their thermal stability. As the temperature increases, the high vibrational mode of molecules in the HSBES system could ameliorate the bond rotation, then destroying the weak interactive bonds between the oxygen atoms of the CMC/KC- NH_4NO_3 HSBES system. Nonetheless, it is worth noting that it helped the migration of H^+ to be decoupled in the CMC/KC backbone, thus exhibiting an increase in ionic conductivity at high temperature, suggesting the correlation between the ionic conductivity and temperature.

Transport properties

To further understand the ionic transport properties of the HSBES system, the ATR-IR deconvolution method was employed to study the ionic distribution in the ATR-IR spectra [45,46]. The asymmetrical $-\text{COO}^-$ of the carboxylate anion group in the CMC-KC biopolymer blend in the ATR-IR spectra was deconvoluted to quantify ion dissociation and association in the HSBES system. The results are illustrated in Fig. 6. As can be observed from the IR spectra, the $-\text{COO}^-$ of the carboxylate anion group in the CMC-KC blend underwent complexation with the NH_4NO_3 , resulting in band shifting as shown in the peak, which is in agreement with the findings of [47,48].

The areas of deconvoluted peaks were carried out by using the Gaussian function, and the band was fitted using the Origin Lab 8.0 software to investigate the outcome of the $-\text{COO}^-$ group in the CMC-KC biopolymer blend with increasing

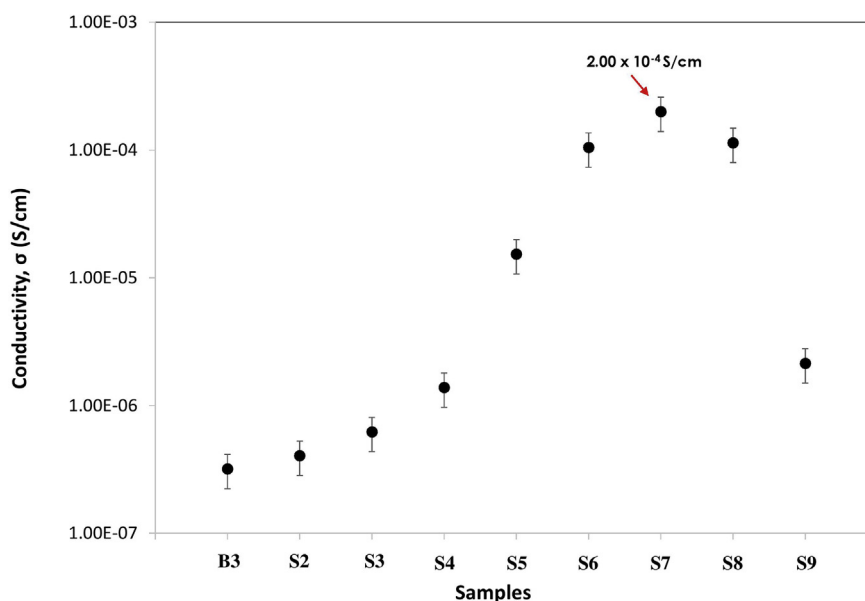


Fig. 4 – Ionic conductivity of the CMC-KC- NH_4NO_3 HSBES system at ambient temperature.

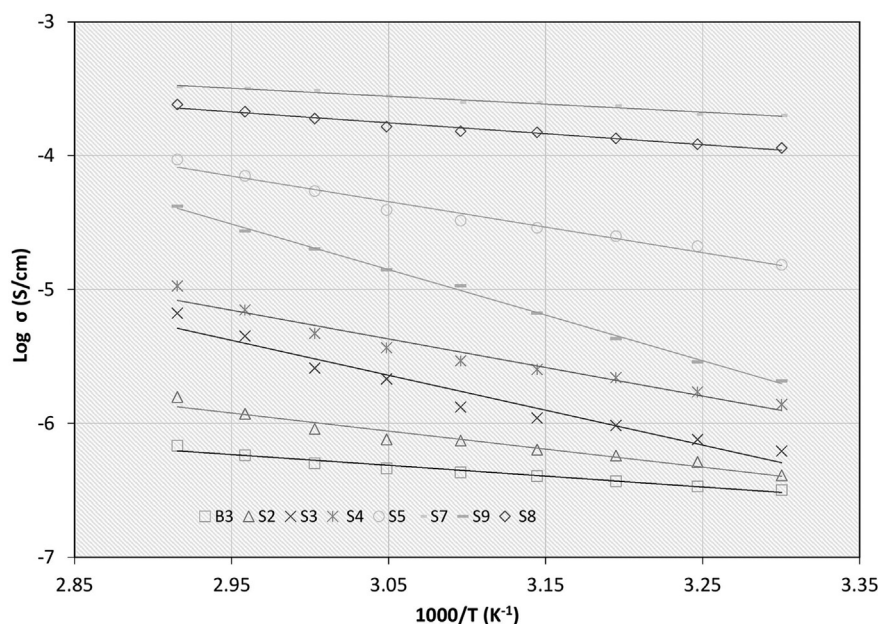


Fig. 5 – Temperature dependence of CMC-KC doped with NH_4NO_3 .

NH_4NO_3 composition as depicted in Fig. 6. The free ions and contact ions of the peaks were assigned from the deconvoluted peaks where the characteristic peak of free ions is larger than that of contact ions as observed by other researchers which using similar method [43,49]. The percentage of free ions were evaluated on the basis of interaction between COO^- to the H^+ from NH_4NO_3 where the presence of free ions (H^+) can be observed from a strong band of COO^- group. This result suggests that the COO^- moieties are highly susceptible to the H^+ and promote the ion migration which could enhance the ionic conductivity [50]. In the present work, the increased filling of NH_4NO_3 are expected to provide huge amount of free ions from the dissociation of $\text{H}^+ - \text{NH}_3$ which was depicted by

sample S2 to S7. However, beyond addition of 30 wt % NH_4NO_3 , the coordination of free ions has decreased due to the enhancement in number of contact ions as quantified by ion-pairs or ion-aggregates ($\text{NH}_4^+ - \text{NO}_3^-$) [49,50]. The area of interest was used between the $1500 - 1700 \text{ cm}^{-1}$ wavenumbers, because the band at $\sim 1581 \text{ cm}^{-1}$ was assigned to the COO^- which has strong affinity with the free ions H^+ whereas the bands at $\sim 1600 \text{ cm}^{-1}$ were attributed to the contact ion-pairs of the ammonium salt system as observed by other previous report [49–53].

The free ions and contact ions of the peaks were calculated from the deconvoluted peaks [43] based on the following equation:

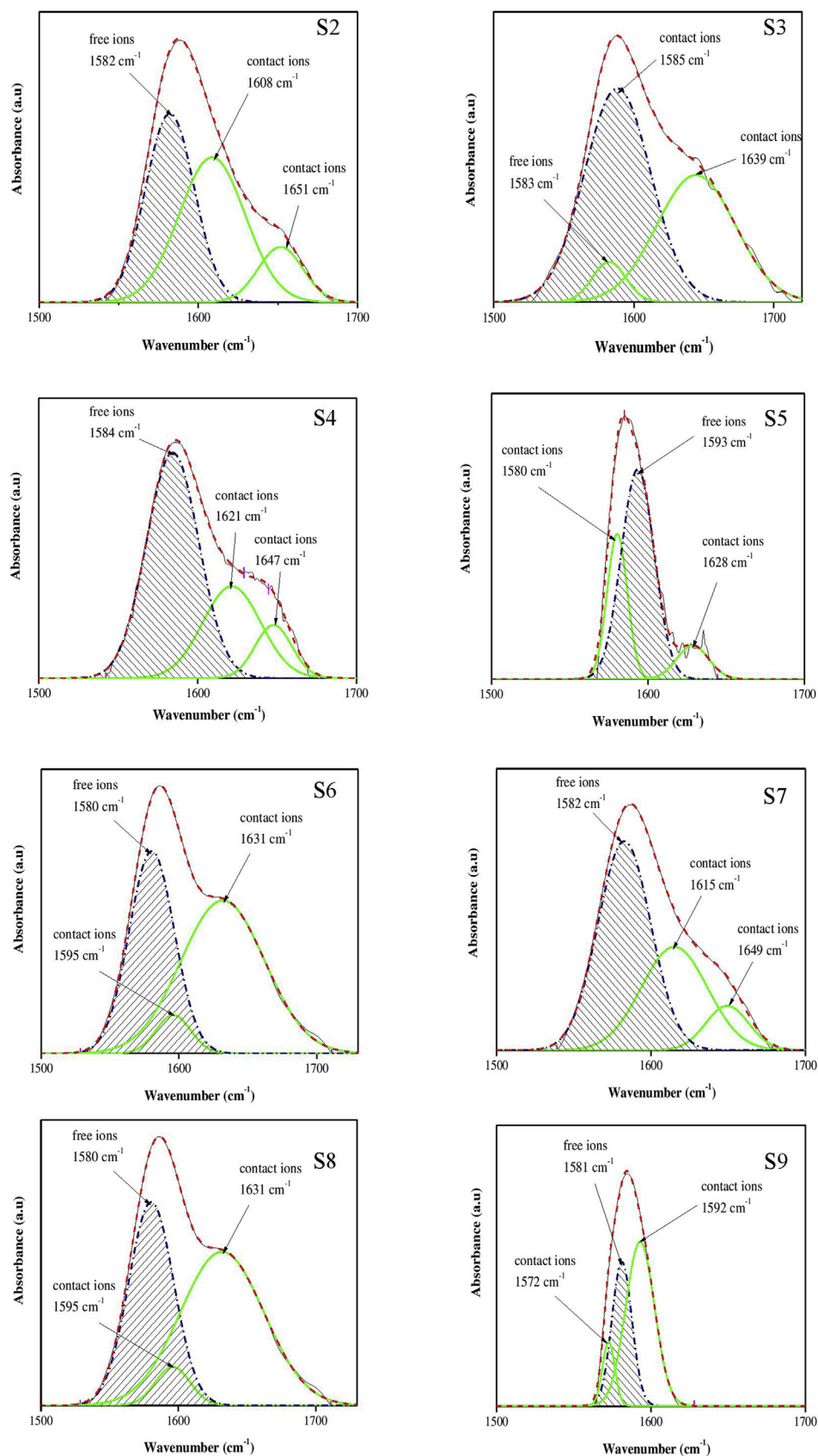


Fig. 6 – IR-deconvolution for various samples of HSBEs.

$$\text{Free ions (\%)} = \frac{A_f}{A_f + A_c} \times 100\% \quad (3)$$

where A_c is the total area under the peak that corresponds to the contact ions region and A_f is the area under the peak that corresponds to the free ions region. Table 1 illustrates the fraction of free ions and contact ions in percentage for HSBES sample.

It can be observed from the table that the free ions band area was at the maximum for the 30 wt% of NH_4NO_3 (sample S7), thus recording the highest ionic conductivity. This suggested that the dissociation of NH_4NO_3 increased the free ion percentage, thereby allowing a more natural migration of the free ions that led to an increase in the number of mobile ions and also ionic conductivity [54]. At higher amounts of NH_4NO_3 , the congregation of free ions was reduced because of the formation of more ion aggregates and hence, the ionic conductivity was decreased. The ionic conductivity did not increase at a similar rate as the increase in NH_4NO_3 (up to 30 wt %) because the amount of dissociation of the NH_4NO_3 decreased due to the formation of the contact ions. This did not contribute to the ionic conductivity due to the blocking effect that hindered the motion of ions, which arose from the decrease in the amorphous content as was proven in the XRD section [55].

The area of the peak was used to calculate the transport parameters (number of mobile ions, η , ionic mobility, μ , and diffusion coefficient, D). The transport parameters equations are as follows [43]:

$$\eta = \frac{MN_A}{V_{\text{Total}}} \times \text{free ions (\%)} \quad (4)$$

$$V_{\text{Total}} = \left[\frac{\text{weight}}{\text{density}} (\text{CMC} / \text{KC}) \right] + \left[\frac{\text{weight}}{\text{density}} (\text{NH}_4\text{NO}_3) \right] \quad (5)$$

$$\mu = \frac{\sigma}{\eta e} \quad (6)$$

$$D = \frac{KT\mu}{e} \quad (7)$$

where, M = Moles of NH_4NO_3 , N_A = Avogadro constant ($1.602 \times 10^{23} \text{ mol}^{-1}$, V_T = Total volume of HSBES, e = electric charge ($1.602 \times 10^{-10} \text{ C}$), k = Boltzmann's constant ($1.38 \times 10^{-23} \text{ J K}^{-1}$) and T = Absolute temperature.

Fig. 7 presents the result of the transport properties of the HSBES system, which were calculated based on the ions fraction. Based on Fig. 7, it can be understood that the increase

in conductivity was governed by the ionic mobility, μ and diffusion coefficient, D , that continued with the increasing NH_4NO_3 , contributing to the highest conductivity of the HSBES at 30 wt% of NH_4NO_3 for sample S7. The rise in the ionic mobility, μ in HSBES was due to the decrement of the crystallinity region (as observed in XRD), resulting in more amorphous areas of the polymer matrix and also supplying a higher number of free conducting pathways. In addition, the dissociation of NH_4NO_3 enhanced the diffusion rate as expected, which caused the linear increase of μ and D . This phenomenon promoted more H^+ of NH_4NO_3 to be protonated towards the COO^- group in the CMC-KC biopolymer blend, as predicted in the FTIR section. Upon blending with the KC, the diffusion coefficient, D , was found to have increased due to the unavailability of loosely entangled H^+ ions with the polymer chains. Furthermore, the increase in ionic mobility, μ and diffusion coefficient, D led to the formation of contact ions, which are electrically neutral, and thus considerably lessened the electrostatic obstacle [56].

Operating potential windows

The potential working windows of the HSBES system for highest conducting sample (S7) was analysed via the linear sweep voltammetry (LSV) method, and the resulting voltammogram is shown in Fig. 8. It can be seen that no noticeable current was recorded from the open-circuit voltage up to $1.96 \pm 0.01 \text{ V}$, which suggested that no electrochemical reaction was observed from this potential window. The plot shows that when the potential reached $2.05 \pm 0.01 \text{ V}$, the current rose dramatically. This can be inferred to the decomposition of the present HSBES sample as reported by other works [57,58]. This observation verified that the present HSBES sample was electrochemically stable up to $2.05 \pm 0.01 \text{ V}$, which was at a similar range as observed by Liew et al. [59]. The authors reported in their work that their highest conducting polyvinyl alcohol (PVA) and ammonium acetate ($\text{CH}_3\text{COONH}_4$) polymer electrolytes sample achieved the electrochemical stability at $\sim 2.2 \text{ V}$ and could be used in electrical double layer capacitors (EDLC). Hence, the potential observation windows showed that the present HSBES system is viable for the construction of an EDLC device.

EDLC characteristics

In the present work, cyclic voltammetry (CV) measurement at various sweep rates from 0 to 1.0 V at room temperature was conducted to evaluate the viability of the HSBES system, particularly sample S7 in an EDLC. Fig. 9 shows the CV plot of the fabricated EDLC at different scan rates. Based on Fig. 9, the shape of the plot changed to a nearly rectangular pattern as the scan rate decreased, with no observable peak, indicating that no redox reaction had occurred in the potential range of 0–1 V [60]. Shuhaimi et al. [61] stated that a rectangular pattern in the CV plot is the shape of an ideal capacitor behaviour within the same potential range while the non-appearance of a peak is caused by non-Faradaic reactions.

The rectangular pattern of the CV curve was an indication of a fast-current reaction to the applied potential. The behaviour of the CV plot in the present work is comparable to

Table 1 – Percentage of free and contact ions of CMC-KC- NH_4NO_3 HSBES.

Sample	Free ions (%)	Contact ions (%)
S2	43.33	56.67
S3	45.63	54.37
S4	53.51	46.49
S5	55.47	44.26
S6	61.77	38.23
S7	63.25	36.75
S8	39.28	60.72
S9	34.28	65.72

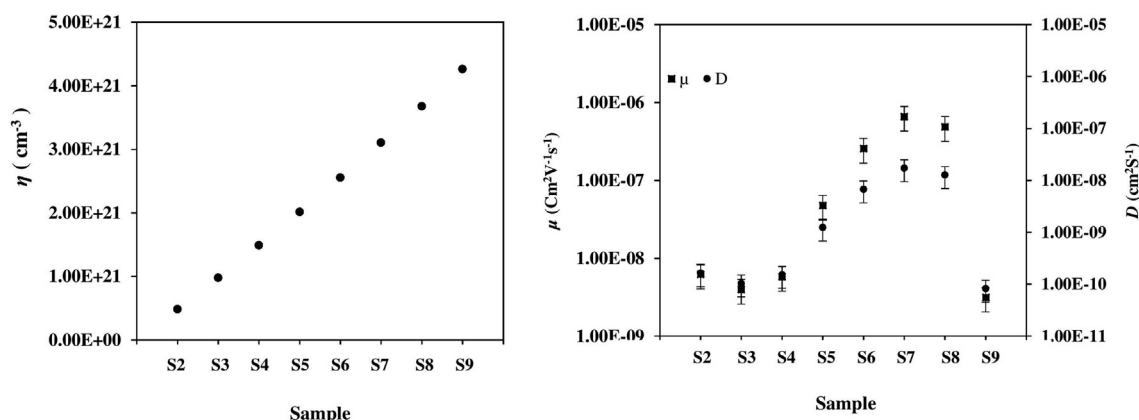


Fig. 7 – Ionic transports properties of HSBEs.

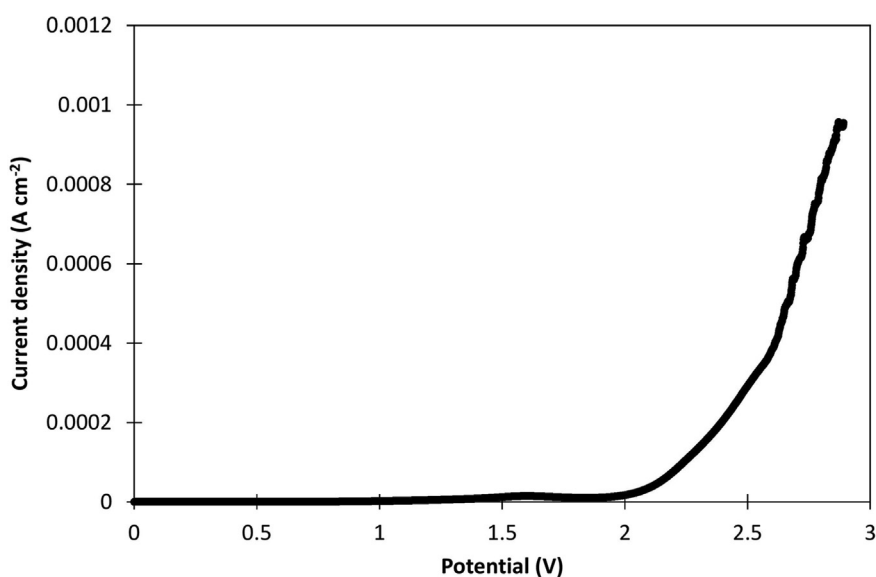


Fig. 8 – Potential windows plot for sample S7.

other EDLC devices of other published works [62]. The non-appearance of reduction and oxidation peaks in the CV pattern at a decreasing scan rate proved that no intercalation/de-intercalation had occurred in the device. This indicated that the behaviour of the fabricated EDLC device was due to the rapid ion diffusion in the HSBEs and ion adsorption towards the interface of electrolyte-electrode and also the accretion of a charge double-layer at the interface of the active materials, namely the active carbon. This indicated that the H^+ ions from the complexes of the HSBEs sample and electrons from the electrodes formed into probable energy as previously reported [63].

Based on the CV plot, the specific capacitance (C_s) values were calculated based on equation (2) and were tabulated as presented in the inset table in Fig. 9. The value of C_s increased as the scan rate decreased, with the highest value of C_s being $\sim 25.83 \text{ F/g}$ for the scan rate of 2 mV/s . As the EDLC devices used an aluminium sheet as a current collector, the superior electrochemical performance of the present sample at the

lower scan rate could be due to a better interface compatibility. The appropriate swelling behaviour of the HSBEs sample greatly facilitated the H^+ charge carrier between the electrolyte and electrodes as illustrated in Scheme 2. This observation could also be due to the ability of H^+ to operate at the entire vacant sites in the active material, thus increasing the C_s .

Galvanostatic charge-discharge (GCD) cycling was carried out in the potential range of $0\text{--}1 \text{ V}$ at different current densities and is shown in Fig. 10 (a). From the plots, it seemed that the values of internal resistance ($I_{R \text{ drop}}$) increased with the increasing current density during charge-discharge. The GCD profiles were almost triangular, which revealed the capacitive nature of the fabricated EDLC up to 1.0 V . However, the GCD profile at a high current density slightly deviated from ideal behaviour, with a larger I_R . The rapid potential drop upon discharge was attributed to the internal resistance (I_R) caused by resistance from the crosslinked structure between the electrode and the present HSBEs as discovered by other

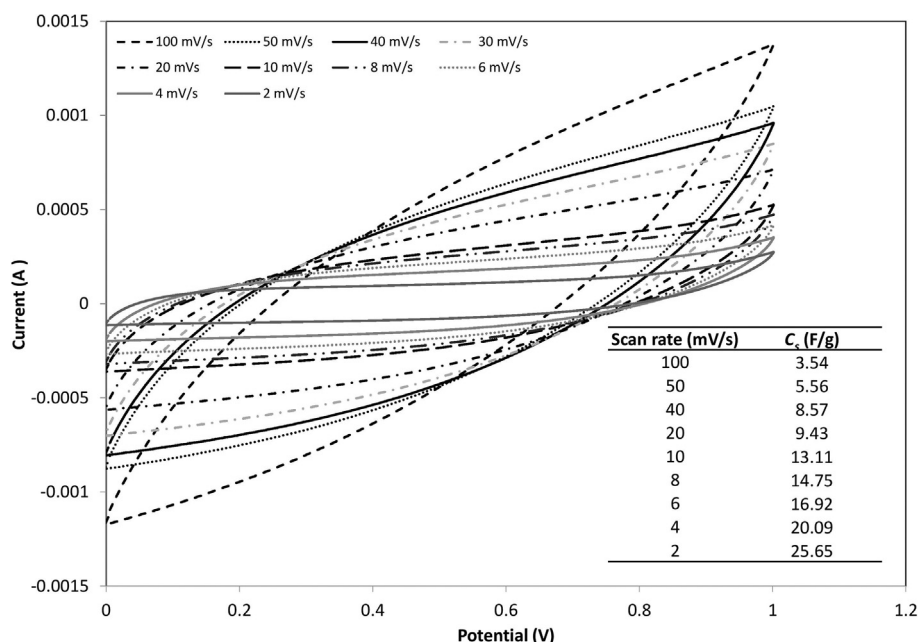


Fig. 9 – Cyclic voltammograms and specific capacitance, C_s of the EDLC at different scan rates.

researchers [61,64]. This explanation can be substantiated via the ohm law equation:

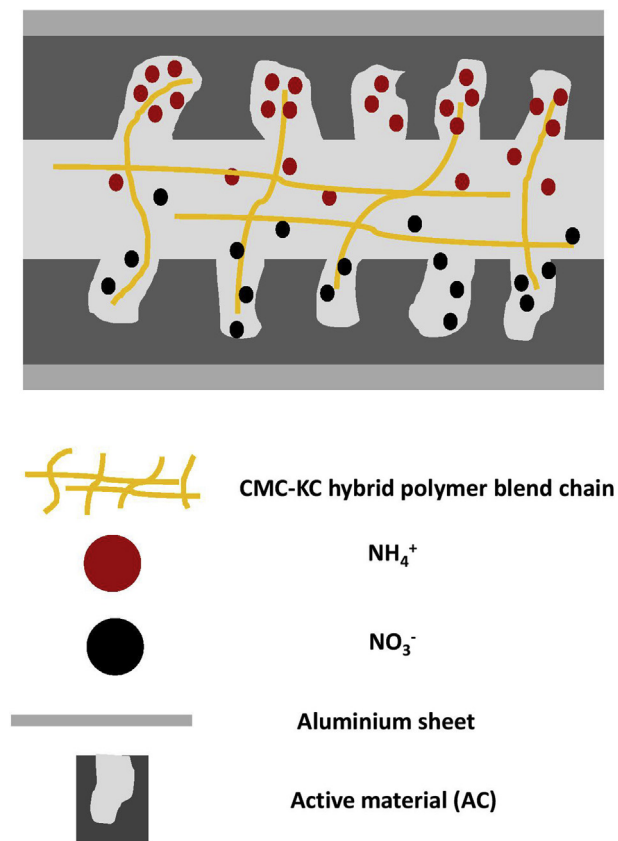
$$V_{\text{cell}} = V_{\text{oc}} - I_{\text{R cell}}, \quad (8)$$

where V_{oc} is the maximum voltage when the circuit is open

and R is the resistance of the EDLC. Based on the equation, the voltage of the present EDLC was proportional to the current and resistance values. Therefore, it is important to reduce the resistance of the EDLC to minimize the $I_{\text{R drop}}$.

The charge-discharge profile of the fabricated EDLC at 0.2 mA cm^{-2} for the selected cycle up to 10000th cycles is shown in Fig. 10 (b). It could be seen that the discharge slope is almost linear, suggesting the existence of capacitive behaviour between the present HSBes at the surface of the electrodes [41]. Based on the charge and discharge pattern, the values of specific capacitance, C_s , equivalent series resistant, ESR and the Coulombic efficiency, η % were calculated and are shown in Fig. 11.

It was noticeable that the C_s was almost constant up to the 10000th cycles with an average of $\sim 20 \text{ F/g}$ with ESR values in the range of $0.7\text{--}1.12 \text{ k}\Omega$. It is well-known that the C_s value of EDLCs depends on the ionic conductivity of the electrolyte itself as reported in the literature [42,65–67] attained value of C_s in the present work is comparable with other reported works for polymer-based electrolytes as tabulated in Table 2. In the inset of Fig. 11, the GCD profile of the 10000th cycle showed a slight deviation compared to that of the first cycle, which indicated that the present EDLC device had good cycling stability with an average Coulombic efficiency of $\sim 95\%$ that revealed the intimate electrolyte-electrode interaction. The persistent stability of the fabricated EDLC showed that it used almost the same time for the charging and discharging processes. Beyond the 1st cycle of charging and discharging, the specific capacitance was increased up to a maximum level with a minimum value of ESR. All of these parameters were expected to decrease afterwards, as the device endures charge and discharge processes. The results thus demonstrate that the CMC-KC HSBes system, which is assisted by the H^+ carrier from the NH_4NO_3 has excellent electrochemical and chemical stabilities energy storage device applications.



Scheme 2 – Illustration of ion migration at the interface between the HSBEs and electrodes in the EDLC device.

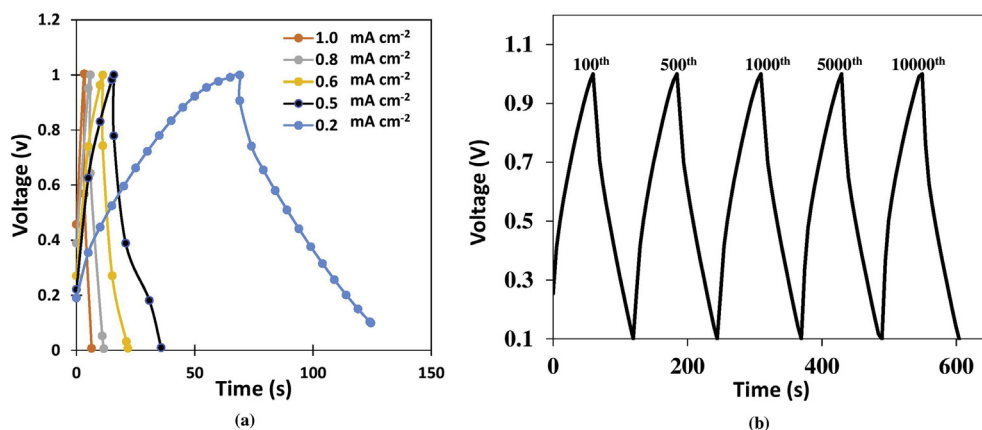


Fig. 10 – (a) Charge-discharge curves of the EDLC at different current densities and (b) charge-discharge profile at different cycles with a current density of 0.2 mA cm^{-2} .

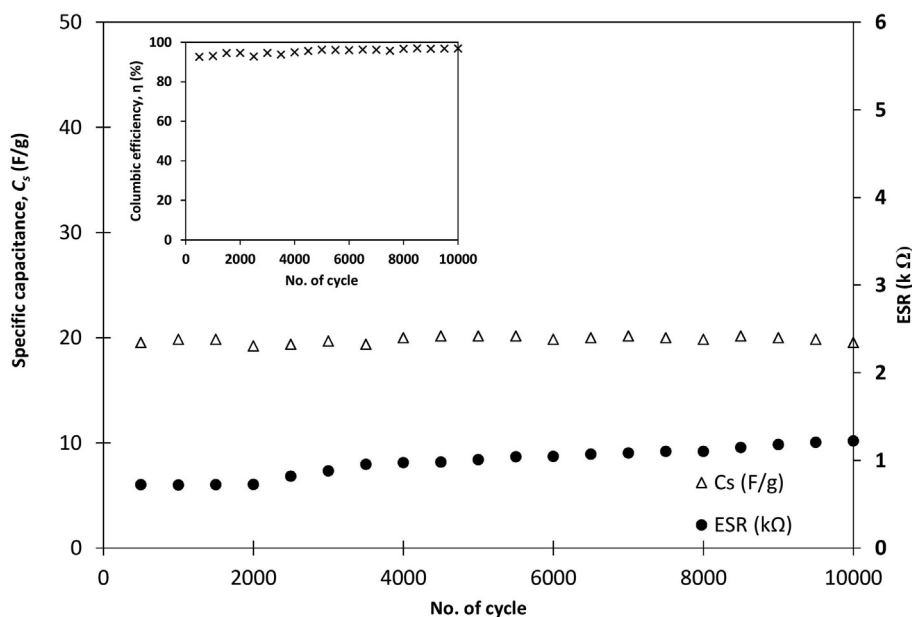


Fig. 11 – Specific capacitance (C_s), equivalent series resistant (ESR) and the Columbic efficiency (η %) of the fabricated EDLC device up to the 10000th cycle.

Table 2 – EDLC properties from literature which using activated carbon as an electrode and polymer electrolytes.

Sample	Specific capacitance, C_s (F/g)	Cycle	References
PVA-CH ₃ COONH ₄ -BmImCl	28.36	500	[42]
Methyl cellulose-potato starch-LiClO ₄ -glycerol	28.04	1000	[65]
Starch-LiOAc-glycerol	33.31	1000	[66]
EC-DMC-LiTFSI-AA	24.01	4000	[67]
CMC-KC-NH ₄ NO ₃	20	10000	Present EDLC

Conclusion

In the present work, proton-conducting hybrid solid biopolymer electrolytes (HSBEs) based on CMC-KC that was doped with various compositions of NH₄NO₃ were successfully prepared using solution casting. The HSBEs samples were characterized by evaluating the structural and ionic conduction properties using Fourier transform infrared (FTIR) spectroscopy, x-ray diffraction (XRD) and electrical impedance spectroscopy (EIS). The complexation between CMC-KC and NH₄NO₃ was confirmed based on the peak spectra changes of the co-ordinating sites in CMC-KC (–OH, C–O–C and COO[–]) via H⁺ bonding. The H⁺ which originated from H⁺–NH₃ group of

NH_4NO_3 is believed to act as carriers for conducting ions that led to the increment in the amorphous phase as revealed by the XRD analysis. The ionic conductivity of HSBES system was found to improve from $\sim 10^{-7}$ and attained the maximum ionic conductivity at ambient temperature at 2.00×10^{-4} S/cm for the sample containing 30 wt % NH_4NO_3 . Based on the IR-deconvolution technique, the present HSBES conduction mechanism was found to be governed by ionic mobility and diffusion coefficient. The EDLC fabricated from the highest conducting HSBES sample (S7) exhibited good electrochemical performance. It displayed a stable cycle performance up to the 10000th cycles with an average specific capacitance (C_s) of ~ 20 F/g from the charge-discharge profile and ~ 25 F/g based on the cyclic voltammetry analysis. Based on the results, it is believed that the present CMC-KC- NH_4NO_3 HSBES system has a great potential to be used in the preparation of polymer electrolytes of electrochemical storage devices.

Acknowledgements

The authors give gratitude to Ministry of Higher Education (MOHE) Malaysia for the financial via FRGS grant (RDU 1901114) and Universiti Malaysia Pahang for internal grant (RDU 190389), Faculty of Industrial Sciences and Technology, University Malaysia Pahang for the technical and facilities given in this work.

Appendix A. Supplementary data

Supplementary data to this article can be found online at <https://doi.org/10.1016/j.ijhydene.2020.01.038>.

REFERENCES

- [1] Gualous H, Bouquain D, Berthon A, Kauffmann J. Experimental study of supercapacitor serial resistance and capacitance variations with temperature. *J Power Sources* 2003;123:86–93.
- [2] Karaman B, Bozkurt A. Enhanced performance of supercapacitor based on boric acid doped PVA-H₂SO₄ gel polymer electrolyte system. *Int J Hydrogen Energy* 2018;43:6229–37.
- [3] Liew C-W, Ramesh S, Arof AK. Characterization of ionic liquid added poly(vinyl alcohol)-based proton conducting polymer electrolytes and electrochemical studies on the supercapacitors. *Int J Hydrogen Energy* 2015;40:852–62.
- [4] Mirzaeian M, Abbas Q, Ogwu A, Hall P, Goldin M, Mirzaeian M, et al. Electrode and electrolyte materials for electrochemical capacitors. *Int J Hydrogen Energy* 2017;42:25565–87.
- [5] Mundinamani S. The choice of noble electrolyte for symmetric polyurethane-graphene composite supercapacitors. *Int J Hydrogen Energy* 2019;44:11240–6.
- [6] Mindemark J, Lacey MJ, Bowden T, Brandell D. Beyond PEO—alternative host materials for Li⁺-conducting solid polymer electrolytes. *Prog Polym Sci* 2018;81:114–43.
- [7] Lamberti A, Fontana M, Bianco S, Tresso E. Flexible solid-state CuxO-based pseudo-supercapacitor by thermal oxidation of copper foils. *Int J Hydrogen Energy* 2016;41:11700–8.
- [8] Shamsudin I, Ahmad A, Hassan NH, Kaddami H. Biopolymer electrolytes based on carboxymethyl κ-carrageenan and imidazolium ionic liquid. *Ionics* 2016;22:841–51.
- [9] Khair ASA, Arof AK. Electrical properties of starch/chitosan- NH_4NO_3 polymer electrolyte. *WASET* 2011;59:23–7.
- [10] Jithunsa M, Tashiro K, Nunes SP, Chirachanchai S. Poly (acrylic acid-co-4-vinylimidazole)/Sulfonated poly (ether ether ketone) blend membranes: a role of polymer chain with proton acceptor and donor for enhancing proton transfer in anhydrous system. *Int J Hydrogen Energy* 2011;36:10384–91.
- [11] Kim DJ, Lee HJ, Nam SY. Sulfonated poly (arylene ether sulfone) membranes blended with hydrophobic polymers for direct methanol fuel cell applications. *Int J Hydrogen Energy* 2014;39:17524–32.
- [12] Zakaria NA, Yahya SYS, Isa MIN, Nor Sabirin M, Subban RHY. Conductivity and dynamic mechanical studies of PVC/PEMA blend polymer electrolytes. *Trans Tech Publ*; 2010.
- [13] Jinisha B, Femy AF, Ashima MS, Jayalekshmi S. Polyethylene oxide (PEO)/polyvinyl alcohol (PVA) complexed with lithium perchlorate (LiClO_4) as a prospective material for making solid polymer electrolyte films. *Mater Today: Proceedings* 2018;5:21189–94.
- [14] Takahashi T, Iwahara H. Solid-state ionics: protonic conduction in perovskite type oxide solid solutions. *Chemischer Informationsdienst* 1981;12:no.
- [15] Colomban P. Proton conductors and their applications: a tentative historical overview of the early researches. *Solid State Ion* 2019;334:125–44.
- [16] Deraman SK, Subban RHY, Nor Sabirin M. Ionic conductivity of PVC-NH₄I-EC proton conducting polymer electrolytes. In: *Advanced materials research*. Trans Tech Publ; 2012. p. 312–6.
- [17] Noor N, Isa M. Investigation on transport and thermal studies of solid polymer electrolyte based on carboxymethyl cellulose doped ammonium thiocyanate for potential application in electrochemical devices. *Int J Hydrogen Energy* 2019;44:8298–306.
- [18] Ahmad NH, Isa MIN. Structural and ionic conductivity studies of CMC based polymerelectrolyte doped with NH_4Cl . *Adv Mater Res* 2015;1107:247–52.
- [19] Rani MSA, Dzulkurnain NA, Ahmad A, Mohamed NS. Conductivity and dielectric behavior studies of carboxymethyl cellulose from kenaf bast fiber incorporated with ammonium acetate-BMATFSI biopolymer electrolytes. *Int J Polym Anal Charact* 2015;20:250–60.
- [20] Mazuki NF, Fuzlin AF, Saadiah MA, Samsudin AS. An investigation on the abnormal trend of the conductivity properties of CMC/PVA-doped NH_4Cl -based solid biopolymer electrolyte system. *Ionics* 2019;25:2657–67.
- [21] Ahmad NH, Isa MIN. Ionic conductivity and electrical properties of carboxymethyl cellulose- NH_4Cl solid polymer electrolytes. *J Eng Sci Technol* 2016;11:839–47.
- [22] Zainuddin N, Saadiah M, Abdul Majeed A, Samsudin A. Characterization on conduction properties of carboxymethyl cellulose/kappa carrageenan blend-based polymer electrolyte system. *Int J Polym Anal Charact* 2018;23:321–30.
- [23] Dorraji MS, Ahadzadeh I, Rasoulifard M. Chitosan/polyaniline/MWCNT nanocomposite fibers as an electrode material for electrical double layer capacitors. *Int J Hydrogen Energy* 2014;39:9350–5.
- [24] Selvakumar M. Multilayered electrode materials based on polyaniline/activated carbon composites for supercapacitor applications. *Int J Hydrogen Energy* 2018;43:4067–80.
- [25] Kadir MFZ, Aspanut Z, Majid SR, Arof AK. FTIR studies of plasticized poly (vinyl alcohol)–chitosan blend doped with

- NH₄NO₃ polymer electrolyte membrane. *Spectrochim Acta A Mol Biomol Spectrosc* 2011;78:1068–74.
- [26] Hema M, Selvasekarapandian S, Arunkumar D, Sakunthala A, Nithya HFTIR. FTIR, XRD and ac impedance spectroscopic study on PVA based polymer electrolyte doped with NH₄X (X= Cl, Br, I). *J Non-Cryst Solids* 2009;355:84–90.
- [27] Guo L, Sato H, Hashimoto T, Ozaki Y. FTIR study on hydrogen-bonding interactions in biodegradable polymer blends of poly (3-hydroxybutyrate) and poly (4-vinylphenol). *Macromolecules* 2010;43:3897–902.
- [28] Mejenom AA, Hafiza MN, Mohamad Isa MIN. X-Ray diffraction and infrared spectroscopic analysis of solid biopolymer electrolytes based on dual blend carboxymethyl cellulose-chitosan doped with ammonium bromide. *ASM Sci J Special Issue* 2018;11:37–46.
- [29] Kamarudin KH, Isa MIN. Structural and DC Ionic conductivity studies of carboxy methylcellulose doped with ammonium nitrate as solid polymer electrolytes. *Int J Phys Sci* 2013;8:1581–7.
- [30] Hashmi SA, Kumar A, Maurya KK, Chandra S. Proton-conducting polymer electrolyte. I. The polyethylene oxide+ NH₄ClO₄ system. *J Phys D Appl Phys* 1990;23:1307.
- [31] Abdullah OG, Aziz SB, Rasheed MA. Incorporation of NH₄NO₃ into MC-PVA blend-based polymer to prepare proton-conducting polymer electrolyte films. *Ionics* 2018;24:777–85.
- [32] Wu HB, Chan MN, Chan CK. FTIR characterization of polymorphic transformation of ammonium nitrate. *Aerosol Sci Technol* 2007;41:581–8.
- [33] Prokhorov E, Luna-Bárcenas G, González-Campos J, Kovalenko Y, García-Carvajal Z, Mota-Morales J. Proton conductivity and relaxation properties of chitosan-acetate films. *Electrochim Acta* 2016;215:600–8.
- [34] Hema M, Selvasekarapandian S, Arunkumar D, Sakunthala A, Nithya H. FTIR, XRD and ac impedance spectroscopic study on PVA based polymer electrolyte doped with NH₄X (X= Cl, Br, I). *J Non-Cryst Solids* 2009;355:84–90.
- [35] Samsudin R AS, Mohamad Isa MIN, Samsudin AS. Ion conducting mechanism of carboxy methylcellulose doped with ionic dopant salicylic acid based solid polymer electrolytes. *Int J Appl Sci Technol* 2012;2:113–21.
- [36] Srivastava N, Chandra S. Studies on a new proton conducting polymer system: poly (ethylene succinate)+ NH₄ClO₄. *Eur Polym J* 2000;36:421–33.
- [37] Samsudin AS, Isa MIN. Structural and ionic transport study on CMC doped NH₄Br: a new types of biopolymer electrolytes. *J Appl Sci* 2012;12:174–9.
- [38] Lutkenhaus J. A radical advance for conducting polymers. *Science* 2018;359:1334–5.
- [39] Deshmukh K, Basheer Ahamed M, Deshmukh RR, Khadheer Pasha SK, Bhagat PR, Chidambaram K. 3 - biopolymer composites with high dielectric performance: interface engineering. In: Sadasivuni KK, Ponnammam D, Kim J, Cabibihan JJ, AlMaadeed MA, editors. *Biopolymer composites in electronics*. Elsevier; 2017. p. 27–128.
- [40] Buraidah M, Teo L, Majid S, Arof A. Ionic conductivity by correlated barrier hopping in NH₄I doped chitosan solid electrolyte. *Phys B Condens Matter* 2009;404:1373–9.
- [41] Lim C-S, Teoh K, Liew C-W, Ramesh S. Electric double layer capacitor based on activated carbon electrode and biodegradable composite polymer electrolyte. *Ionics* 2014;20:251–8.
- [42] Liew C-W, Ramesh S, Arof A. Good prospect of ionic liquid based-poly (vinyl alcohol) polymer electrolytes for supercapacitors with excellent electrical, electrochemical and thermal properties. *Int J Hydrogen Energy* 2014;39:2953–63.
- [43] Arof AK, Amirudin S, Yusof SZ, Noor IM. A method based on impedance spectroscopy to determine transport properties of polymer electrolytes. *Phys Chem Chem Phys* 2014;16:1856–67.
- [44] Aziz NN, Idris N, Isa M. Proton conducting polymer electrolytes of methylcellulose doped ammonium fluoride: conductivity and ionic transport studies. *Int J Phys Sci* 2010;5:748–52.
- [45] Dey A, Karan S, Dey A, De S. Structure, morphology and ionic conductivity of solid polymer electrolyte. *Mater Res Bull* 2011;46:2009–15.
- [46] Noor I, Majid S, Arof A. Poly (vinyl alcohol)–LiBOB complexes for lithium–air cells. *Electrochim Acta* 2013;102:149–60.
- [47] Chai M, Isa M. Novel proton conducting solid bio-polymer electrolytes based on carboxymethyl cellulose doped with oleic acid and plasticized with glycerol. *Sci Rep* 2016;6:27328.
- [48] Che Balian S, Ahmad A, Mohamed N. The effect of lithium iodide to the properties of carboxymethyl κ-carrageenan/ carboxymethyl cellulose polymer electrolyte and dye-sensitized solar cell performance. *Polymers* 2016;8:163.
- [49] Hafiza M, Isa M. Correlation between structural, ion transport and ionic conductivity of plasticized 2-hydroxyethyl cellulose based solid biopolymer electrolyte. *J Membr Sci* 2019;117176.
- [50] Ramli M, Isa M. Structural and ionic transport properties of proton conducting solid biopolymer electrolytes based on carboxymethyl cellulose doped with ammonium fluoride. *J Phys Chem B* 2016;120:11567–73.
- [51] Ramya C, Selvasekarapandian S, Savitha T, Hirankumar G, Angelo P. Vibrational and impedance spectroscopic study on PVP–NH₄SCN based polymer electrolytes. *Phys B Condens Matter* 2007;393:11–7.
- [52] Rajeswari N, Selvasekarapandian S, Sanjeeviraja C, Kawamura J, Bahadur SA. A study on polymer blend electrolyte based on PVA/PVP with proton salt. *Polym Bull* 2014;71:1061–80.
- [53] Woo H, Majid SR, Arof AK. Conduction and thermal properties of a proton conducting polymer electrolyte based on poly (ε-caprolactone). *Solid State Ion* 2011;199:14–20.
- [54] Sohaiimy MIH, Isa MIN. Conductivity and dielectric analysis of cellulose based solid polymer electrolytes doped with ammonium carbonate (NH₄CO₃). In: *Applied mechanics and materials*. Trans Tech Publ; 2015. p. 67–72.
- [55] Rajeswari N, Selvasekarapandian S, Karthikeyan S, Sanjeeviraja C, Iwai Y, Kawamura J. Structural, vibrational, thermal, and electrical properties of PVA/PVP biodegradable polymer blend electrolyte with CH₃COONH₄. *Ionics* 2013;19:1105–13.
- [56] Arof AK, Naeem M, Hameed F, Jayasundara WJMJSR, Careem MA, Teo LP, et al. Quasi solid state dye-sensitized solar cells based on polyvinyl alcohol (PVA) electrolytes containing I⁻/I₃⁻ redox couple. *Opt Quant Electron* 2014;46:143–54.
- [57] Kadir MFZ, Arof AK. Application of PVA–chitosan blend polymer electrolyte membrane in electrical double layer capacitor. *Mater Res Innov* 2011;15:217–20.
- [58] Noor NAM, Isa MIN. Investigation on transport and thermal studies of solid polymer electrolyte based on carboxymethyl cellulose doped ammonium thiocyanate for potential application in electrochemical devices. *Int J Hydrogen Energy* 2019;44:8298–306.
- [59] Liew C-W, Ramesh S, Arof AK. Enhanced capacitance of EDLCs (electrical double layer capacitors) based on ionic liquid-added polymer electrolytes. *Energy* 2016;109:546–56.
- [60] Aziz SB, Hamsan MH, Kadir MF, Karim WO, Abdullah RM. Development of polymer blend electrolyte membranes based on chitosan: dextran with high ion transport properties for EDLC application. *Int J Mol Sci* 2019;20:3369.
- [61] Shuhaimi NEA, Teo LP, Woo HJ, Majid SR, Arof AK. Electrical double-layer capacitors with plasticized polymer

- electrolyte based on methyl cellulose. *Polym Bull* 2012;69:807–26.
- [62] Aziz SB, Hamsan M, Karim WO, Kadir M, Brza M, Abdullah OG. High proton conducting polymer blend electrolytes based on chitosan: dextran with constant specific capacitance and energy density. *Biomolecules* 2019;9:267.
- [63] Kang J, Wen J, Jayaram SH, Yu A, Wang X. Development of an equivalent circuit model for electrochemical double layer capacitors (EDLCs) with distinct electrolytes. *Electrochim Acta* 2014;115:587–98.
- [64] Pandey G, Kumar Y, Hashmi S. Ionic liquid incorporated PEO based polymer electrolyte for electrical double layer capacitors: a comparative study with lithium and magnesium systems. *Solid State Ion* 2011;190:93–8.
- [65] Yusof Y, Shukur M, Hamsan M, Jumbri K, Kadir M. Plasticized solid polymer electrolyte based on natural polymer blend incorporated with lithium perchlorate for electrical double-layer capacitor fabrication. *Ionics* 2019:1–12.
- [66] Shukur M, Ithnin R, Kadir M. Electrical characterization of corn starch-LiOAc electrolytes and application in electrochemical double layer capacitor. *Electrochim Acta* 2014;136:204–16.
- [67] Nadiah NS, Omar FS, Numan A, Mahipal YK, Ramesh S, Ramesh K. Influence of acrylic acid on ethylene carbonate/dimethyl carbonate based liquid electrolyte and its supercapacitor application. *Int J Hydrogen Energy* 2017;42:30683–90.